Appl Nanosci (2012) 2:409–415
DOI 10.1007/s13204-011-0053-9

ORIGINAL ARTICLE

Compositional variation of magnetic moment, magnetic anisotropy energy and coercivity in $Fe_{(1-x)}M_x$ (M = Co/Ni) nanowires: an ab initio study

S. Assa Aravindh · S. Mathi Jaya · M. C. Valsakumar · C. S. Sundar

Received: 28 October 2011 / Accepted: 27 December 2011 / Published online: 8 January 2012

Abstract Ab initio simulations are used to investigate the magnetic and electronic properties of freestanding $Fe_{(1-x)}M_x$ (M = Co/Ni) nanowires. The stability of the nanowires increases with Co (Ni) addition, as seen from the increase in cohesive energy. With the addition of Co (Ni), the average magnetic moment shows a monotonic decrease, in contrast to the Slater–Pauling behavior observed in bulk Fe–Co/Ni alloys. The magnetic anisotropy energy of the nanowire is observed to change sign, from a parallel alignment of spins along the wire axis, to a perpendicular alignment with the increase of Co and Ni content. The magnetic anisotropy energy variation is seen to be correlated with the orbital moment anisotropy. The coercivity, as calculated using the Jacobs–Bean model is observed to decrease with Co (Ni) addition to the nanowire.

Keywords $Fe_{(1-x)}Co_x$ and $Fe_{(1-x)}Ni_x$ nanowires · Magnetic moment · Magnetic anisotropy energy · Coercivity · Ab initio calculations

Introduction

The magnetic properties of nanowires, which are substantially different from the bulk, can be tuned with changes in diameter, aspect ratio and composition of the constituent materials (Sellmyer and Skomski 2005; Mills and Bland 2006). For example, in the nanowire configuration, the magnetic moment, magnetic anisotropy energy (MAE) and coercivity are considerably enhanced—offering the potential of applications in magnetic recording and nanoscale devices. Of particular interest is the variation of magnetic properties of transition metal alloy nanowires—with changes in composition. A variety of experimental studies on the magnetic properties of Fe–Co (Qin et al. 2003; Lee et al. 2003; Chen et al. 2003; Zhan et al. 2002) and Fe–Ni (Kashi et al. 2010; Liu et al. 2005) nanowires have been carried out. While all these studies point to the improved magnetic properties, since these are experiments on nanowires of different diameter, and prepared by different methods, an unambiguous systematic on the trends in the variation of magnetic properties with composition is yet to emerge.

On the theoretical front too, there have been several investigations (Jo et al. 2005; Jo 2009; Tung and Guo 2007; Hong and Wu 2003; Lazarovits et al. 2003; Kishi et al. 2004; Sabirianov 2006) focusing on the magnetic properties of transition metal nanowires. For example, Tung and Guo (2007) investigated the magnetic and electronic structure of 3d transition metal atomic chains, linear and zig-zag, using ab initio techniques and they observed magnetic moment and MAE enhancement in Fe, Co and Ni nanowire from that of the corresponding bulk value. Binding energy, magnetic moments and coercivity of $Fe_{1-x}Co_x$ alloy nanowires with bcc (001) orientation have been carried out using ab initio simulations (Jo et al. 2005; Jo 2009) to show that the coercivity and magnetic moments are enhanced from the bulk alloy values.

In the present study, we report a systematic study on the compositional variation of cohesive energy, magnetic moment, and magnetic anisotropy energy in $Fe_{(1-x)}Co_x$ and $Fe_{(1-x)}Ni_x$ nanowires using first principles simulations. All the calculations have been performed for bcc (110)

S. Assa Aravindh (✉) · S. Mathi Jaya · M. C. Valsakumar · C. S. Sundar
Materials Physics Division, Materials Science Group, Indira Gandhi Centre for Atomic Research, Kalpakkam 603102, Tamil Nadu, India
e-mail: assa@igcar.gov.in; mails2asa@gmail.com

oriented nanowires following the experimental results that, $Fe_{(1-x)}Co_x$ and $Fe_{(1-x)}Ni_x$ nanowires prefer bcc (110) orientation (Chen et al. 2003; Lee et al. 2003; Liu et al. 2005; Qin et al. 2003; Yue et al. 2009a, b; Zhan et al. 2002). We have seen that the cohesive energy of the nanowires increase with Co (Ni) content. The values of magnetic moments calculated using spin-polarized calculations indicate a monotonic decrease with Co (Ni) content, which is at variance with the well-known Slater–Pauling behavior seen in bulk alloys (Bozorth 1951; Soderlind et al. 1992). The paper also addresses the issue of variation of magnetic anisotropy energy with composition using non-collinear calculations (Marsman and Hafner 2002) and correlated with anisotropy of orbital moment (Bruno 1989).

Calculational details

The freestanding isolated nanowires are constructed by periodic repetition of a supercell made up of bcc (110) atomic planes stacked along the *Z*-direction. Periodic boundary conditions are assumed along the *Z*-direction and a vacuum region of 15 Å is used in the *X* and *Y* directions to ensure negligible interaction between the images. The *a*, *b* and *c* lattice parameters of the unit cell is defined as, $a = \sqrt{(2)} \times a_0$, $b = a_0$ and $c = 2a_0$, in accordance with bcc (110) planes. The value of a_0 is taken as 2.866 Å, which is the bulk bcc Fe lattice parameter. The alloying of Fe and Co/Ni atoms in the $Fe_{(1-x)}Co_x$ and $Fe_{(1-x)}Ni_x$ (where $x = 0$–1) nanowires are done randomly to generate the various compositions. The calculations are performed within the framework of density functional theory, as implemented in the VASP package (Kresse and Furthmuller 1996). The projector-augmented wave method (PAW) is used to describe the electron–ion interactions (Kresse and Joubert 1999). The PW91, which is a semi-local functional in the generalized gradient approximation (GGA) is used to describe the electronic exchange and correlation (Perdew and Wang 1992). Structural optimization of the $Fe_{(1-x)}Co_x$ and $Fe_{(1-x)}Ni_x$ nanowires are carried out employing the conjugate gradient algorithm as implemented in VASP. Optimization runs are stopped when the Hellmann–Feynman forces become smaller than 10 meV/Å and the total energies of nanowires are calculated within a tolerance of 10^{-7} eV. For the Brillouin zone integration $2 \times 2 \times 20$ Monkhorst–Pack **k**-point grid is used (Monkhorst and Pack 1976). A plane wave cut-off energy of 450 eV is used for the plane waves included in the basis set. Spin-polarized calculations to get the magnetic properties are described using the spin interpolation proposed by Vosko et al. (1980). The tetrahedron method with Blochl corrections is used for the DOS calculations (Blochl et al. 1994). Spin–orbit coupling scheme used is that of Kresse and Lebacq as implemented in the VASP. The non-collinear calculations are performed using the prescription by Hobbs et al. (2000) and Marsman and Hafner (2002). The magnetic anisotropic energy (MAE) is obtained from the difference in total energies corresponding to the parallel and perpendicular orientation of the magnetization with respect to the axis of the nanowire. The calculations for the MAE are performed in two steps. A collinear scalar relativistic calculation was done initially and the ground state that resulted out of this calculation is used to initialize the noncollinear calculation including spin–orbit coupling (Marsman and Hafner 2002). Orbital magnetic moments are calculated directly from the wave functions as the expectation value of the components for the angular momentum operator along the direction of magnetization.

Cohesive energy

The nanowires constructed using the supercell technique are subjected to structural optimization and $Fe_{(1-x)}M_x$ nanowire corresponding to $x = 0.5$ is shown in the inset of Fig. 1. In order to study the stability of these nanowires with respect to the change in composition, we have calculated the cohesive energy/atom and which is defined as:

$$E_C = \frac{(-E_{\text{total}} + n_{\text{Fe}}E_{\text{Fe}} + n_{\text{M}}E_{\text{M}})}{(n_{\text{Fe}} + n_{\text{M}})} \quad (1)$$

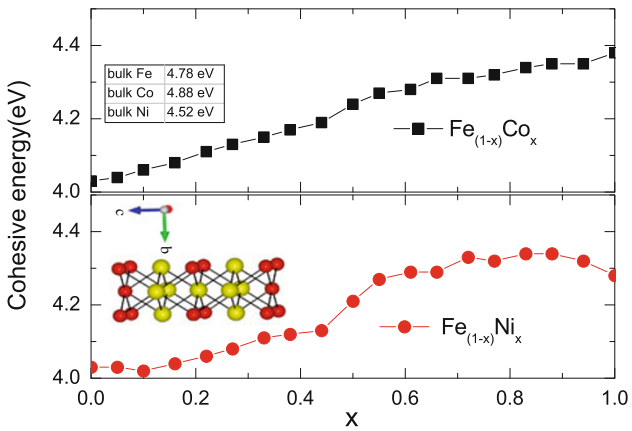

Fig. 1 The cohesive energy of $Fe_{(1-x)}Co_x$ and $Fe_{(1-x)}Ni_x$ nanowires as a function of composition. The bulk cohesive energy values of bcc Fe, hcp Co and fcc Ni are 4.78, 4.88 and 4.52 eV, respectively, as calculated by GGA–PBE potentials (from Philipsen and Baerends 1996) are shown in the *table inside the plot*. The individual nanowires of Fe, Co and Ni shows less stability than the bulk counterparts, the increase in cohesive energy at high concentrations of Co and Ni indicate that stability of nanowires increase with respect to Co and Ni alloying. The *inset* shows the structure of $Fe_{(1-x)}M_x$ nanowire with $x = 0.5$

where M = Co or Ni, E_{Fe} is the energy corresponding to a free Fe atom, and E_M is that of a Co or Ni atom. The free atom energies are calculated by the cubic box supercell approach with the cell size of 10 Å. E_{total} is the total energy corresponding to the $Fe_{(1-x)}Co_x$ or $Fe_{(1-x)}Ni_x$ nanowires consisting of n_{Fe} or n_M atoms, respectively. The calculated values of the cohesive energies are shown in Fig. 1. For comparison, the cohesive energy for bulk Fe, Co and Ni are 4.78, 4.88 and 4.52 eV, as calculated using GGA–PBE potentials (Philipsen and Baerends 1996), are indicated inside the table in the Fig 1. It is noted that the cohesive energies of pure Fe, Co and Ni nanowires, viz., 4.03, 4.38 and 4.28 eV, respectively, are smaller than that of bulk counterparts. This is reasonable as nanowires, having more exposed surface atoms are having low coordination number compared to bulk, which in turn reduces the cohesive energy. Further, it is seen from Fig. 1 that there is a systematic increase in the cohesive energy of Fe–Co/Ni alloy nanowires with the addition of Co and Ni. The binding energy of Fe–Co nanowire calculated by Jo (2009) follows the same trend, viz., an increase with Co content. The values calculated by Jo (2009) are slightly lower, viz., −3.0 eV, and this may be related to the fact that their calculations are for nanowires with bcc (001) orientation, as against (110) in our case. It must be emphasized that in the present calculations we have only considered nanowires with bcc (110) orientation, and any possible change in the structure with composition has not been considered. The experimental studies on $Fe_{(1-x)}Co_x$ and $Fe_{(1-x)}Ni_x$ nanowires showed bcc (110) orientation for these nanowires for a large concentration range of Fe, and the structural change occur at very high concentrations (above 80%) of Co or Ni. (Chen et al. 2003; Lee et al. 2003; Liu et al. 2003; Yue et al. 2009a, b; Zhan et al. 2002). Further there is a study which reports no change in structure and the $Fe_{(1-x)}Co_x$ nanowire showed bcc (110) for the entire concentration range (Qin et al. 2003). Our choice of bcc (110) orientation for the nanowires was dictated from the above mentioned experimental results.

Magnetic moments

To study the magnetic moments, we have performed spin-polarized calculations for various compositions ($x = 0$–1) of the $Fe_{(1-x)}Co_x$ and $Fe_{(1-x)}Ni_x$ nanowires, and these results are shown in Fig. 2. The average magnetic moments (M_s) are calculated as $M_s = xS_M + (1 - x)S_{Fe}$ where S_{Fe} and S_M are the individual spin magnetic moment of Fe and Co/Ni, respectively. The spin moments of Fe, Co and Ni in the nanowire configuration are seen to be 2.6, 1.8 and 0.8 μ_B, respectively, as compared to their bulk values of

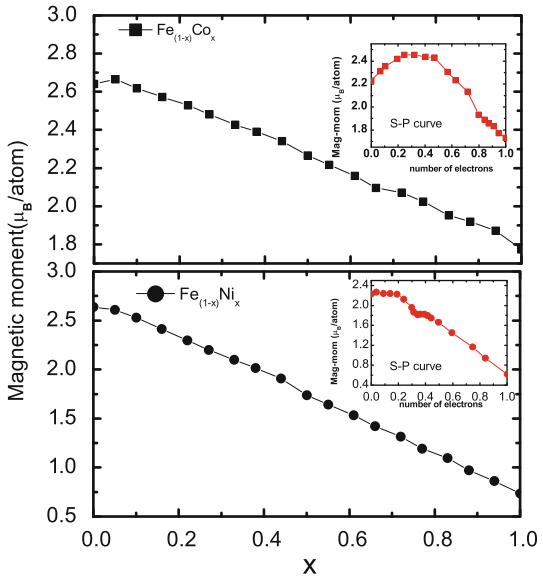

Fig. 2 The average spin magnetic moment of $Fe_{(1-x)}Co_x$ and $Fe_{(1-x)}Ni_x$ alloy nanowires along with the corresponding Slater–Pauling curve (shown in the *inset*; data taken from Bozorth 1951) for bulk Fe–Co and Fe–Ni alloys. It can be seen that for both the nanowires, the magnetic moment falls with composition, showing deviation from Slater–Pauling behavior

2.2, 1.72 and 0.6 μ_B (Stearns 1986). It can be seen that the magnetic moment of Fe nanowire is enhanced considerably compared to the bulk value, whereas that of Co and Ni nanowires do not show significant enhancement. A similar trend of increase in magnetic moment of Fe nanowire and bulk-like value for Co and Ni nanowire is also seen by Kishi et al. (2004) and explained on the basis of changes in electronic structure due to the narrowing of bands. Now turning to the compositional variation of magnetic moments of the nanowire, we have seen that the average magnetic moments of the alloy nanowires show a monotonic decrease, as compared to the well-known dome-shaped Slater–Pauling curve (Bozorth 1951; Soderlind et al. 1992) seen in bulk alloys. Similar results from deviation of Slater–Pauling behavior is observed in $Fe_{(1-x)}Co_x$ nanowires by Jo (2009), as also in the studies by Moulas et al. (2008) in $Fe_xCo_{(1-x)}$ monolayers in their first principles study. Magnetic circular dichroism study by Wills and Gilman (2005) on "surface sensitive" magnetic moment in binary alloys of transition metals also shows a linear variation with composition as seen in Fig. 2.

The observed monotonic decrease in magnetic moment with the addition of Co/Ni can be understood from the changes in band filling. In Fig. 3 are shown the spin-polarized density of states (DOS) and integrated density of states for $Fe_{17}Co_1$ and $Fe_{13}Co_5$ nanowires, which correspond to low Co content, wherein the magnetization deviates from the Slater–Pauling curve. It can be seen from

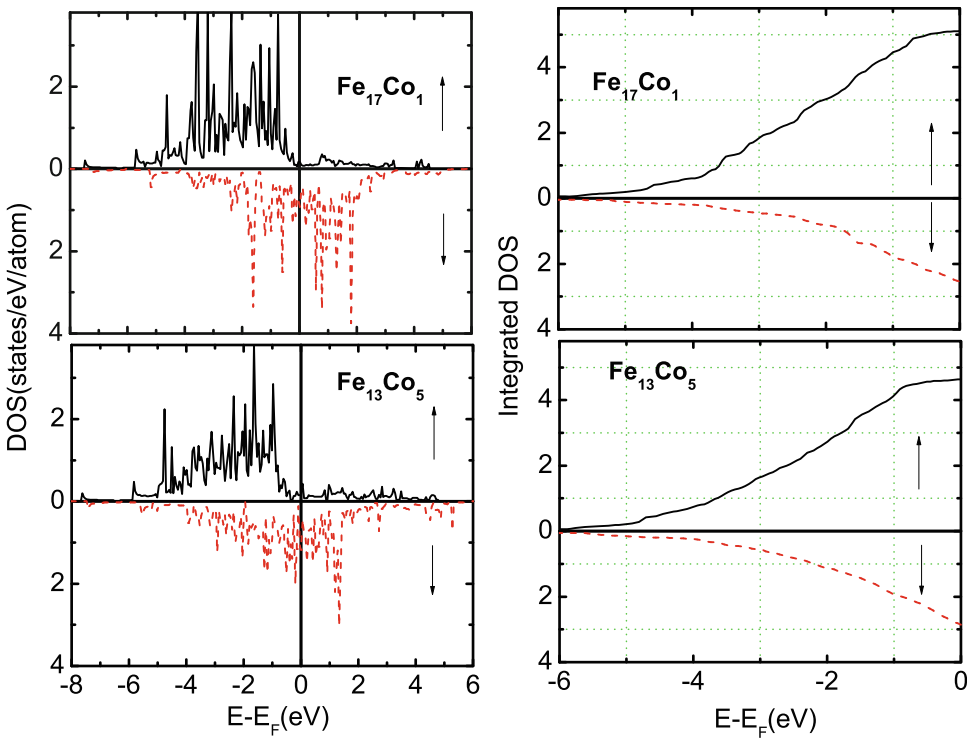

Fig. 3 The density of states (*DOS*) and integrated DOS for the $Fe_{(1-x)}Co_x$ nanowires for two different compositions. Spin-up and spin-down DOS are plotted with *solid* and *dashed lines*, respectively. It can be seen that the DOS and integrated DOS vary with the change in composition of the nanowires. The reduction in magnetic moment with the change in composition can be understood from the difference between the spin-up and spin-down integrated DOS

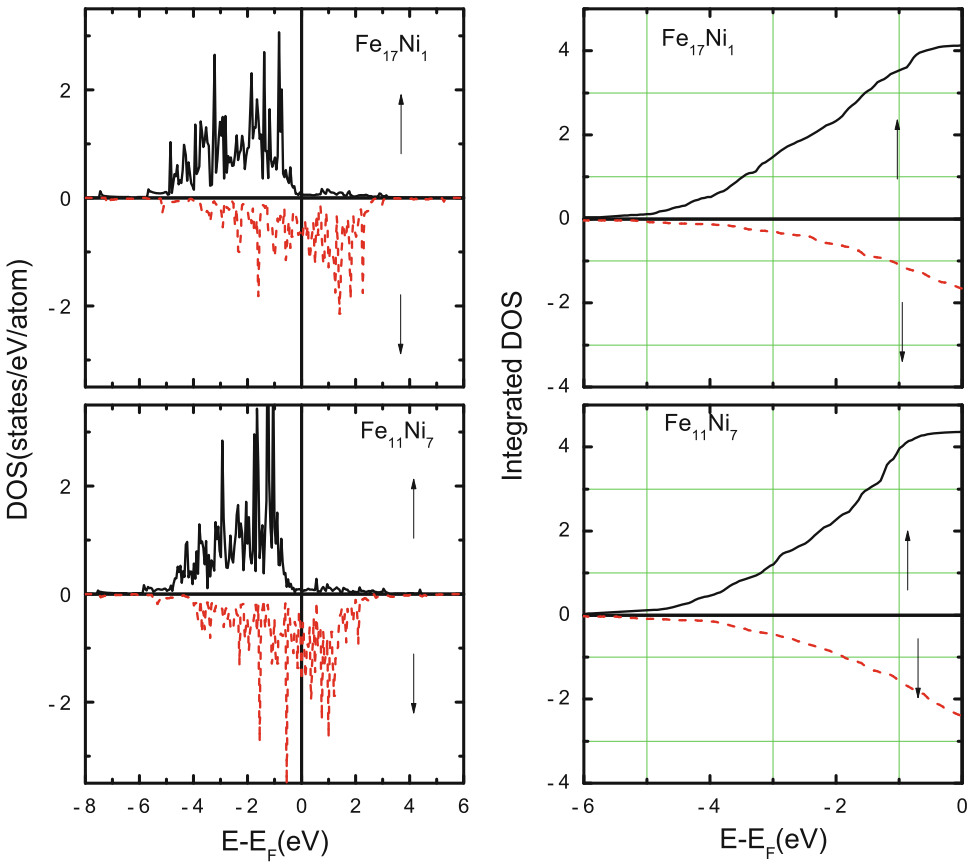

Fig. 4 The density of states (*DOS*) and integrated DOS for the $Fe_{(1-x)}Ni_x$ nanowires for two different compositions. Spin-up and spin-down DOS are plotted with *solid* and *dashed lines*, respectively. It can be seen that the DOS and integrated DOS vary with the change in composition of the nanowires. The reduction in magnetic moment with the change in composition can be understood from the difference between the spin-up and spin-down integrated DOS

the integrated DOS plots that an increase in Co concentration results in a decrease in the majority spin occupation and an increase in the minority spin occupation, leading to a decrease in magnetic moment. This is different from the case of bulk alloy, wherein the initial electrons populate the up-spin states and only beyond 30% of Co, the down-spin

states begin to be occupied. The DOS calculations for the $Fe_{(1-x)}Ni_x$ nanowires is also carried out and the results for two specific compositions ($Fe_{17}Ni_1$ and $Fe_{11}Ni_7$) are shown in Fig. 4. It can be seen from the DOS and integrated DOS plots that the spin-up population is not significantly altered, while the spin-down population significantly increases, causing the magnetic moment to decrease with the addition of Ni.

Magnetic anisotropy energy

The magnetic moments in a magnetic system often align along certain preferred direction with respect to the crystalline axes called the easy axis. The magneto-crystalline anisotropy energy, often referred as magnetic anisotropy energy (MAE) is the energy required to rotate the orientation of magnetic moments from easy axis to hard axis. It is already well known that for transition metal nanowires the shape anisotropy is negligibly small compared to the MAE, which arises from the spin–orbit coupling interactions (Tung and Guo 2007). First principles studies have shown that MAE as large as 0.1 meV/atom is obtained for Co monatomic wires (Hong and Wu 2003). MAE of the order of 0.2 meV/Fe atom and 0.1 meV/Co and Ni atoms are also shown in nanowires of Fe, Co and Ni in first principles LSDA calculations (Luo et al. 2009). The observation of large MAE compared to the corresponding bulk counterparts in the nanowires can be related to the occurrence of increased orbital moments as pointed out by Bruno (1989). We have included the relativistic spin–orbit coupling in our calculations to calculate the MAE and orbital moments of the nanowires for all the compositions studied. Separate simulations are carried out with atomic spins oriented along the nanowire axis (*Z*-axis), and also along the perpendicular direction (*X*-axis).

We define the MAE as, $MAE = E_{\|} - E_{\perp}$, where $E_{\|}$ is the total energy of the nanowire, when all the magnetic moments are aligned along the axis of the nanowire (*Z*-axis). $E_{\perp}$ is the total energy, corresponding to magnetization oriented along the *X*-axis. A positive MAE means that the magnetization prefers to lie along the nanowire axis (*Z*-direction) and a negative MAE indicates that a perpendicular anisotropy is preferred, i.e., the magnetic moments prefer to lie perpendicular to the nanowire axis (*X*-axis). The calculated MAE for the $Fe_{(1-x)}Co_x$ and $Fe_{(1-x)}Ni_x$ nanowires with the change in composition is shown in the Fig. 5. First we note that the MAE of the nanowires are larger than that of the bulk counterparts, as has been already observed in earlier studies (Hong and Wu 2003; Hong 2006; Luo et al. 2009). The MAE values for Fe, Co and Ni nanowires, as obtained from our study are about 0.1, −0.04, and −0.21 meV/atom, which are larger

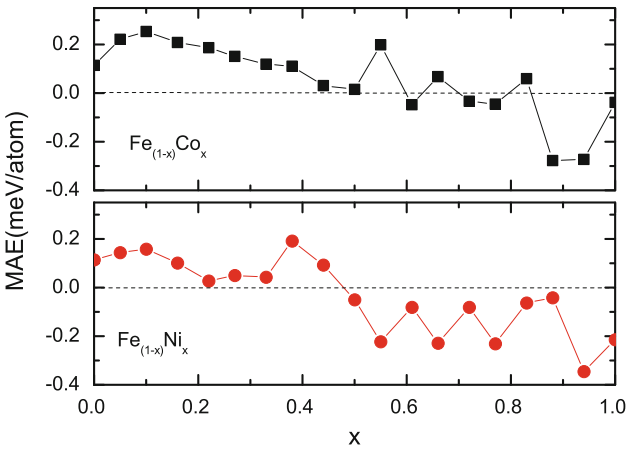

Fig. 5 The variation of MAE with the change in composition of the nanowires. The *lines* are guide to the eyes. It is seen that the MAE becomes negative with increase in *x*, indicating that easy axis of nanowire change from along the axis of the wire to a perpendicular axis

than the corresponding values for bulk Fe (1.4 μeV), Co (45 μeV) and Ni (−2.7 μeV) (Stearns 1986). Further it is seen from Fig. 5 that the sign of MAE and consequently the easy axis of magnetization changes with the change in composition of nanowire. The easy axis of magnetization switches from along the wire for pure Fe to the perpendicular axis with the increase in number of Co and Ni atoms. First principles calculations on Fe linear chains using FLAPW method also showed a preference of chain axis as the easy axis (Hong 2006). The observation of perpendicular magnetic anisotropy in Co nanowires is reported by Sabirianov (2006). The change in magnetization direction in Fe–Co nanowires with the change in Co concentration is observed in different studies (Yue et al. 2009a, b; Qin et al. 2003). A correlation between the MAE and the anisotropy in orbital moment was suggested by Bruno (1989). Following this, we have evaluated the orbital moment anisotropy (Δm_L), defined as $\Delta m_L = m_{L\|} - m_{L\perp}$, where $m_{L\|}$ and $m_{L\perp}$ are the orbital moments calculated along the easy ($m_{L\|}$) and hard axes ($m_{L\perp}$) of magnetization for all the compositions. A plot of MAE versus the orbital moment anisotropy is shown in Fig. 6. It can be seen that the MAE and orbital moment anisotropy show a strong correlation as suggested by Bruno (1989).

Coercivity

Apart from the magnetic moments and magnetic anisotropy energy, an important magnetic property is the coercivity. By changing the alloy composition, the coercivity of the alloy nanowires can be tuned to suit for application purposes. The coercivity of the nanowires were estimated by

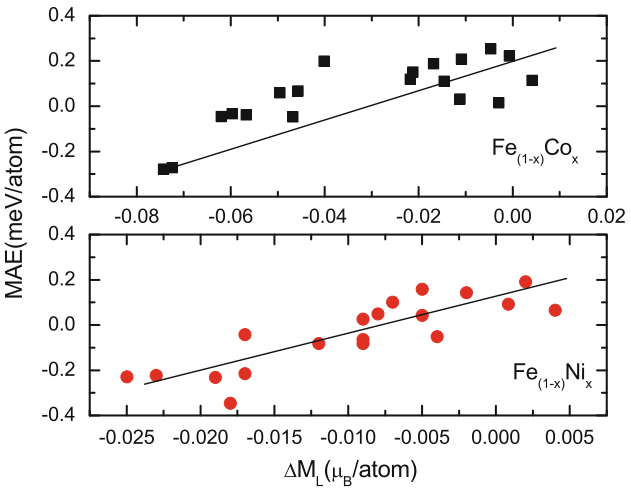

Fig. 6 The MAE versus anisotropy of orbital moments (Δm_L). *Lines* are guide to the eyes. The orbital moments calculated along the easy and hard axes of magnetization are different in magnitude and this anisotropy of orbital moments give rise to the MAE

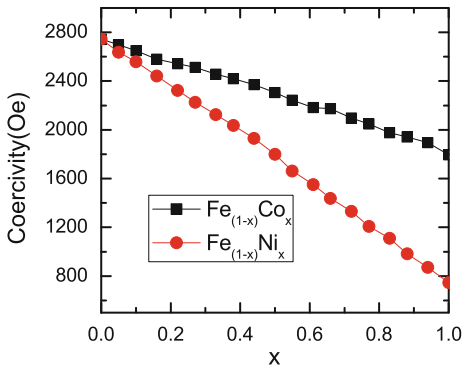

Fig. 7 The coercivity for $Fe_{(1-x)}M_x$ nanowires calculated using the model of Jacobs and Bean (1955). It is seen that the coercivity linearly decreases with the increase in x and hence follows the trend shown by the magnetization of the nanowires

treating the nanowires as a chain of prolate ellipsoids of the same size and the magnetization reversal process of these ellipsoids is described by the symmetric fanning reversal mechanism (Jacobs and Bean 1955; Chen et al. 2003). The coercivity ($H_{c,m}$) of the nanowires are calculated by the following formula (Chen et al. 2003).

$$H_{c,m} = \frac{1}{\alpha^2}\Pi(6M_m + 2L_m)\frac{M_s}{6} + 4\Pi(N_\perp - N_\Pi)M_s. \qquad (2)$$

Here $\alpha = b/a$ is the aspect ratio of the ellipsoid and n is the aspect ratio of the nanowire. We have taken $n = 400$ for our calculations (Jo et al. 2005). We have carried out calculations by varying the value of n and seen that the coercivity of the nanowire, calculated within the framework of the chain of ellipsoids model, increases initially with the aspect ratio of the nanowire, and saturates beyond 400, similar to the trend observed by Chen et al. (2003). M_s is the saturation magnetization of the nanowires and $N_\perp$ and $N_\parallel$ are the demagnetization factors of the ellipsoid, perpendicular and parallel to the axis of the nanowires which depend only on the aspect ratio α of the ellipsoid. The lattice parameters of the bcc (110) oriented nanowire investigated in the present study are $a = 4.053$ Å, $b = 2.866$ Å and $c = 5.7319$ Å. For a chain of ellipsoid model for the nanowire, an ellipsoid with $a = b = 5.7319$ Å and $c = 4.053$ Å was used in our calculations. The calculated coercivity for the $Fe_{(1-x)}Co_x$ and $Fe_{(1-x)}Ni_x$ nanowires are shown in Fig. 7. It can be noted from the figure that the coercivity for the pure Fe, Co and Ni nanowires are about 2,700, 1,800 and 800 Oe, respectively, which are larger than that of bulk values (Fe ~2 Oe, Co ~10 Oe, Ni ~0.7 Oe). It is seen that the coercivity decreases linearly with the increase in composition of Co and Ni. This linear reduction in coercivity with the increase in x is same as the change in magnetization of the nanowires. Experimental and theoretical investigations on the coercivity of Fe–Co nanowire have been carried out by Chen et al. (2003) and Zhan et al. (2002). Similar studies on $Fe_{(1-x)}Ni_x$ nanowires have been carried out by Liu et al. (2005). Studies on 20 nm Fe–Co nanowire indicate that the coercivity increases from 2,400 to 2,800 Oe at 30% Co content, afterwards it decreases, following the trend shown by magnetization. Coercivity calculations, using the chain of spheres model with symmetric fanning, have been carried out with bulk magnetization values for alloys, to account for these experimental observations (Chen et al. 2003; Zhan et al. 2002). In our case, we have used the calculated magnetic moment of the nanowire (cf. Fig. 2), which shows a linear reduction with composition. Since the coercivity is linearly proportional to the saturation magnetization (Eq. 2), this may account for the linear trend in coercivity as seen in Fig. 7. This calls for further experiments on the magnetization and coercivity of narrower nanowires.

Conclusion

In this work, we have calculated the compositional variation of cohesive energy, average magnetic moment, magnetic anisotropy and coercivity for $Fe_{(1-x)}M_x$ (M = Co, Ni) nanowires with bcc (110) orientation, using ab initio simulation methods. With the addition of Co (Ni) the cohesive energy is seen to increase while the magnetic moment and coercivity decreases. The monotonic variation of magnetic moment with composition is at variance with the Slater–Pauling curve seen in bulk alloys. Interestingly, the MAE for nanowires is seen to change sign with composition. The lower Co (Ni) content prefers the parallel alignment of spins along the wire axis, whereas at higher composition, a perpendicular alignment is preferred. The

variation in MAE, which is determined by the spin–orbit interaction, is seen to be correlated with the anisotropy in the orbital moment. The observed trends in cohesive energy, magnetic moment, coercivity and MAE, with varying composition can be exploited in the design of nanowires for applications.

References

Blochl PE, Jepsen O, Anderson OK (1994) Improved tetrahedron method for Brillouin zone integrations. Phys Rev B 49:16223. doi:10.1103/PhysRevB.49.16223

Bozorth RM (1951) Ferromagnetism. Van Nostrand, New York

Bruno P (1989) Tight-binding approach to the orbital magnetic moment and magnetic crystalline anisotropy of transition-metal monolayers. Phys Rev B 39:865. doi:10.1103/PhysRevB.39.865

Chen W, Tang S, Lu M, Du Y (2003) The magnetic properties and reversal of Fe–Co nanowire arrays. J. Phys. Cond. Matt. 15:4623 PII:S0953-8984(03)59002-6

Hobbs D, Kresse G, Hafner J (2000) Fully unconstrained noncollinear magnetism within the projector augmented-wave method. Phys Rev B 62:11556. doi:10.1103/PhysRevB.62.11556

Hong J (2006) Nearly half-metallic one-dimensional Fe atomic chain on NiAl(110) and its magnetic properties. Phys Rev B 73:092413. doi:10.1103/PhysRevB.73.092413

Hong J, Wu RQ (2003) First principles calculations of magnetic anisotropy energy of Co monatomic wires. Phys Rev B 67:020406(R). doi:10.1103/PhysRevB.67.020406

Jacobs IS, Bean CP (1955) An approach to elongated fine-particle magnets. Phys Rev 100:1060. doi:0.1103/PhysRev.100.1060

Jo Ch (2009) Magnetic properties of $Fe_{(1-x)}Co_x$ nanowires inside a (6,6) carbon nanotube. J Phys D Appl Phys 42:105008. doi:10.1088/0022-3727/42/10/105008

Jo Ch, Lee J, Yang Y (2005) Electronic and magnetic properties of ultrathin Fe–Co alloy nanowires. Chem. Mater. 17:2667. doi:10.1021/cm047921j

Kashi MA, Ramazani A, Eshaghi F, Ghanbari S, Esmaeily (2010) Microstructure and magnetic properties in arrays of ac electrodeposited Fe_xNi_{1-x} nanowires induced by the continuous and pulse electrodeposition. Phys B 405:2620. doi:10.1007/s00339-010-5980-x

Kishi T, Kasai H, Nakanishi H, Dino WA, Komori F (2004) Electronic structure of Fe, Co, Ni nanowires on Cu (111). Surf Sci 566:1052. doi:10.1016/j.susc.2004.06.051

Kresse G, Furthmuller J (1996) Efficient iterative schemes for abinitio total-energy calculations using a plane-wave basis set. Phys Rev B 54:11169. doi:10.1103/PhysRevB.54.11169

Kresse G, Joubert D (1999) From ultrasoft pseudopotentials to the projector augmented-wave method. Phys Rev B 59:1758. doi:10.1103/PhysRevB.59.1758

Lazarovits B, Szunyogh L, Weinberger P, Ujfalussy B (2003) Magnetic properties of finite Fe chains at fcc Cu(001) and Cu(111) surfaces. Phys Rev 68:024433. doi:10.1103/PhysRevB.68.024433

Lee GH, Huh SH, Jeong JW, Kim SH, Choi BJ, Ri HC, Kim B, Park JH (2003) Arrays of ferromagnetic FeCo and FeCr binary nanocluster wires. J Appl Phys 94:4179. doi:10.1063/1.1602955

Liu QF, Gao CX, Xiao JJ, Xue DS (2003) Size effects on magnetic properties in Fe0.68Ni0.32 alloy nanowire arrays. J Magn Magn Mater 260:151. doi:10.1016/S0304-8853(02)01315-X

Liu Q, Wang J, Yan Z, Xue D (2005) Characterization and magnetic properties of $Fe_{1-x}Ni_x$ nanowire arrays. Phys Rev B 72:144412. doi:10.1103/PhysRevB.72.144412

Luo SJ, Guo GY, Laref A (2009) Magnetism of 3d-transition metal (Fe, Co, and Ni) nanowires on w-BN (0001). J Phys Chem C 113:14615. doi:10.1021/jp810124k

Marsman M, Hafner J (2002) Broken symmetries in the crystalline and magnetic structures of γ-iron. Phys Rev B 66:224409. doi:10.1103/PhysRevB.66.224409

Mills DL, Bland JAC (2006) Nanomagnetism: ultrathin films, multilayers and nanostructures: contemporary concepts of condensed matter science series. Elsevier

Monkhorst HJ, Pack JD (1976) Special points for Brillouin-zone integrations. Phys Rev B 13:5188. doi:10.1103/PhysRevB.13.5188

Moulas G, Lehnert A, Rusponi S, Zabloudil J, Etx C, Ouazi S, Etzkorn, Bencok P, Gambardella P, Weinberger P, Burne H (2008) High magnetic moments and anisotropies for Fe_xCo_{1-x} monolayers on Pt(111) Phys Rev B 78:214424. doi:10.1103/PhysRevB.78.214424

Perdew JP, Wang Y (1992) Accurate and simple analytic representation of the electron–gas correlation energy. Phys Rev B 45:13244. doi:10.1103/PhysRevB.45.13244

Philipsen PHT, Baerends EJ (1996) Cohesive energy of 3d transition metals: density functional theory atomic and bulk calculations. Phys Rev B 54:5326. doi:10.1103/PhysRevB.54.5326

Qin DH, Peng Y, Cao L, Li HL (2003) A study of magnetic properties: Fe_xCo_{1-x} alloy nanowire arrays. Chem Phys Lett 374:661. doi:10.1016/S0009-2614(03)00809-1

Sabirianov (2006) Magnetic anisotropy and anisotropic ballistic conductance of thin magnetic wires. J Magn Magn Mater 300:136. doi:10.1016/j.mmm.2005.10.050

Sellmyer D, Skomski R (2005) Advanced magnetic nanostructures. Springer

Soderlind P, Erisson O, Johansson B, Albers RC, Boring AM (1992) Spin and orbital magnetism in Fe–Co and Co–Ni alloys. Phys Rev B 45:12911. doi:10.1103/PhysRevB.45.12911

Stearns MB (1986) Alloys and compounds. Springer, Berlin

Tung JC, Guo GY (2007) Systematic ab initio study of the magnetic and electronic properties of all 3d transition metal linear and zigzag nanowires. Phys Rev B 76:094413. doi:10.1103/PhysRevB.76.094413

Vosko SH, Wilk L, Nusair M (1980) Accurate spin-dependent electron liquid correlation energies for local spin density calculations: a critical analysis. Can J Phys 58:1200. doi:10.1139/p80-159

Wills RF, Gilman NJ (2005) Distinguishing magnetic-moment and magnetic-ordering behavior on the Slater–Pauling curve. Euro Phys Lett 69:411. doi:10.1209/epl/i2004-10359-2

Yue GH, Wang LS, Wang X, Chen YZ, Peng DL (2009a) Characterization and magnetic properties of $Fe_{70}Co_{30}$ alloy nanowire arrays. J App Phys 105:074312. doi:10.1063/1.3103775

Yue GH, Wang X, Wang LS, Chang P, Wen RT, Chen YZ, Peng DL (2009b) Structure and magnetic properties of $Fe_{1-x}Co_x$ nanowires in self-assembled arrays. Electro Chim Acta 54:6543. doi:10.1016/j.electacta.2009.06.037

Zhan Q, Chen Z, Xue D, Li F (2002) Structure and magnetic properties of Fe–Co nanowires in self-assembled arrays. Phys Rev B 66:134436. doi:10.1103/PhysRevB.66.134436